



# A viscoelastic approach from $\alpha$ -Al<sub>2</sub>O<sub>3</sub> suspensions with high solids content

Luiz F.G. Setz<sup>a,\*</sup>, Antonio C. Silva<sup>b</sup>, Silas C. Santos<sup>b</sup>,  
Sonia R.H. Mello-Castanho<sup>b</sup>, Márcio R. Morelli<sup>c</sup>

<sup>a</sup> Center for Engineering, Modeling and Applied Social Science, Federal University of ABC, Av. dos Estados 5001, Santo André, SP 09210-580, Brazil

<sup>b</sup> Materials Science and Technology Center, Nuclear and Energy Research Institute, Av. Lineu Prestes, 2242 Cidade Universitária, Sao Paulo, SP 05508-900, Brazil

<sup>c</sup> Department of Materials Engineering, Federal University of São Carlos, Rodovia Washington Luís, km 235, Sao Carlos, SP 13565-905, Brazil

Received 1 March 2013; received in revised form 14 May 2013; accepted 4 June 2013

Available online 27 June 2013

## Abstract

The flow properties of high solids concentration suspensions has been extensively studied and established, however, the rheological behavior for ceramics suspensions with very high solids loading, up to 60 vol.% is poorly known. This is due to both difficulties of preparation and behavior measurement. The theory shows ceramics suspensions with very high solids loading may present viscoelastic properties attributed to interparticle forces active. The oscillatory and creep-recovery rheological measurements can provide this knowledge when discretion used. Thus, rheological behavior of alumina suspensions with high solids loading (>43 vol.%), properly stabilized and the characterization of slip casting shaped samples has been analyzed. High solids loading suspensions, over 43 vol.%, present adequate flow and suspensions with solid content since 60 vol.% present viscoelastic properties attributed to interparticle forces active. The rheological parameters can provide subsidies to obtain after shaping process, such as extrusion, injection and plastic pressing, suitable products for the desired application.

© 2013 Elsevier Ltd. All rights reserved.

**Keywords:** Rheology; Viscoelasticity; Alumina; Colloidal processing.

## 1. Introduction

The rheological behavior of ceramic suspensions has been widely studied and therefore well established. The requirements conditions for the several shaping processes, such as, slip casting, tape casting, gel casting, dip coating, etc. may vary depend on each technique, however, all these shaping methods are based on dispersed concentrates suspension, generally below 80 wt.% of solids. High concentrations of solids are usually necessary to reduce both drying problems and shaping time.<sup>1</sup> However, when the solids concentration in those stable suspensions, is elevated beyond the usual values (~80 wt.%), the responses become more forceful to provide. This is due to particles proximity; consequence of the interparticle forces active, repulsive electrostatic forces and attractive (London – van der Waals), generating high viscosity and elastic effect.

Structured liquids have a natural ground condition in which their microstructure represents a minimum-energy state. When those liquids are deformed, thermodynamic forces immediately begin to operate to restore their ground state, for example, as stretched spring will always seek to return to its unextended length. Similarly as a spring, movement from the ground state represents storage of energy, which manifests itself as an elastic force trying to reproduce the initial static condition. This kind of energy is the source of the elasticity in structured liquids.

The elastic force exhibits itself in small deformations between various elastic moduli, such as the storage modulus (linear region), and at steady state (i.e. very large deformations) by a normal-stress difference, as Weissenberg effect, in the non-linear elastic region.<sup>2</sup> Besides those elastic forces, the viscous force is an ever-present due to the dissipation, proportion and the rate not extent of deformation; therefore together they produce viscoelastic effects. For a long times, linear viscoelastic effect has been confused with thixotropy, however the difference between both is that under the linear viscoelastic region the microstructure over responds in a restricted time scale without changing. Otherwise, the thixotropic property does change

\* Corresponding author. Tel.: +55 11 4996 7940.

E-mail addresses: [luiz.setz@ufabc.edu.br](mailto:luiz.setz@ufabc.edu.br), [lfsetz@yahoo.com.br](mailto:lfsetz@yahoo.com.br) (L.F.G. Setz).

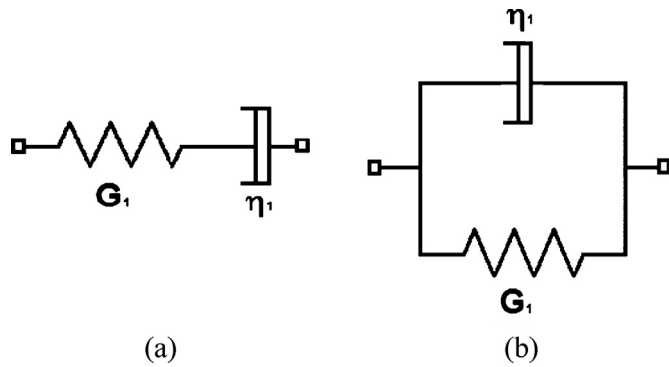


Fig. 1. Viscoelastic mechanical model: Maxwell (a) and Kelvin-Voigt (b).

the microstructure, by breaking down or building up and such changes take as a function of the time.<sup>3</sup>

The viscoelasticity understanding is done by using of simple mechanical models. These models consist of combinations of linear elastic and viscous elements, i.e. springs and dashpots (Fig. 1). A spring is a representation of a linear elastic element that follows Hooke's law, i.e. the strain is proportional of applied stress ( $\sigma$ ). In a simple shear deformation ( $\gamma$ ) the constant of proportionality is the elastic modulus ( $G$ ), Eq. (1).

$$\sigma = G\gamma \quad (1)$$

It is important to notice that time does not considered into this behavior, so that, if a strain is applied ( $\gamma$ ) to unstrained model, the resultant stress ( $\sigma$ ) suddenly appears, and then, if the strain is removed, the stress ( $\sigma$ ) falls immediately to zero (and vice versa when a stress is applied). Similarly, linear viscous response can be displayed using a dashpot. A plunger moving through a very viscous Newtonian liquid physically is an example of this model. The response of this element is described mathematically by the Eq. (2).

$$\sigma = \eta \dot{\gamma} \quad (2)$$

Only the rate of deformation matters, and if switched on an stress  $\sigma$ , the dashpot immediately starts to deform and continue deforming at a constant deformation rate  $\dot{\gamma}$  and without any change with time until the stress is removed, and then the deformation stops immediately (once again vice versa if a shear rate

is applied). There are no effects of the time. If a spring and a dashpot are connect in series, the simplest representation of a viscoelastic liquid is obtained, and this arrangement is called a Maxwell model (Fig. 1a). If a single elastic and viscous elements are connect in parallel, they end up with the simplest representation of a viscoelastic solid, and this procedure has been named Kelvin-Voigt model (Fig. 1b).

The viscoelasticity, which are considered in processes such as injection and extrusion, can be determined by oscillatory rheological measurements and through curves and creep-recovery,<sup>4</sup> however, due to the inherent difficulties of preparing and making measurement of ceramic suspensions above 80 wt.% of solids, viscoelasticity in ceramic suspensions is virtually unknown, and thus the aim of this work is to investigate the viscoelastic behavior of stable alumina suspensions with high solids concentration.

## 2. Experimental procedure

A high purity  $\alpha$ -Al<sub>2</sub>O<sub>3</sub> powder (Almatis, A1000, USA), with specific surface area of 8.2 m<sup>2</sup> g<sup>-1</sup> (BET – Monosorb, Quantachrome, USA) and average particle size of 0.67  $\mu$ m (SediGraph 5000ET, Micromeritics, USA) (Fig. 2) has been used. The particles morphology was observed in Scanning Electronic Microscopic (SEM – Quanta 600FEG, FEI Company, USA).

The stability of the  $\alpha$ -Al<sub>2</sub>O<sub>3</sub> powders was studied as a function of pH through Zeta potential measurements, which were performed using Phase Analysis Light Scattering (ZetaPALS, Brookhaven Instruments Corporation, USA). The samples were prepared with solid content of 0.01 vol.% in deionized water (Milli-Q Plus pure). The ionic strength was fixed at 10<sup>-3</sup> M using KNO<sub>3</sub> (Aldrich-Chemie, Germany) as indifferent electrolyte. The pH adjustments were made by adding appropriate amounts of HNO<sub>3</sub> and KOH. For results standardization, all suspensions were ultrasonicated for 1 min to homogenize the sample.

Suspensions of  $\alpha$ -Al<sub>2</sub>O<sub>3</sub> powder were prepared in deionized water with solids concentration of 42–63 vol.%. Dispersion was achieved by adding 0.2 wt.% of citric acid related to the dry solids, according to previous works.<sup>5,6</sup> To reduce powder

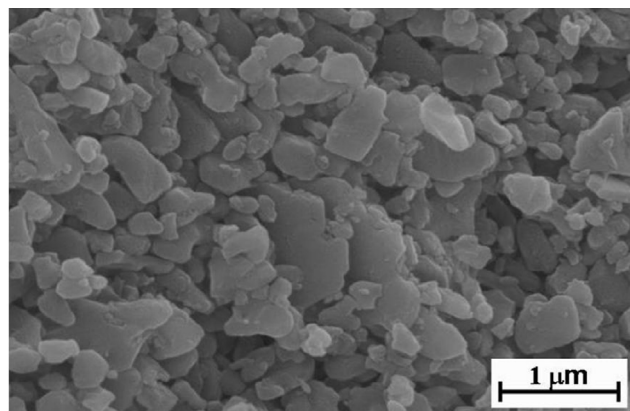
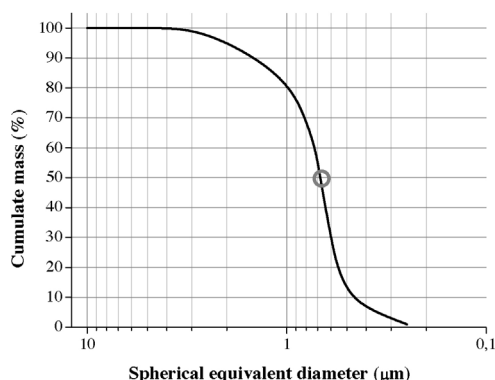


Fig. 2.  $\alpha$ -Al<sub>2</sub>O<sub>3</sub> powders SEM micrograph and average particle size.

agglomerates, the slurries were ball milled for times up to 24 h, using alumina balls.

The rheological behaviour of all prepared slurries was performed through a rheometer (Haake RS600, Thermo, Germany) able to operate at either controlled shear rate (CR), controlled shear stress (CS) and oscillatory modes (OSC). The used sensors systems were a double-cone rotor and a stationary plate. This system being surrounded by a cylindrical wall, the chamber is protected with a solvent trap to reduce evaporation phenomena (CR and CS) a plate-plate rotor was used for OSC and Creep-Recovery measurements. The flow curves were determined by controlled rate mode (CR) in order to characterizing the slurry stability. Measurements were performed by increasing the shear rate from 0 to  $1000\text{ s}^{-1}$  in 5 min, and maintaining at  $1000\text{ s}^{-1}$  for 2 min and returning to 0 in 5 min. CS measurements were achieved by increasing the stress from 0 to a value higher than the yield point estimated by direct observations of the CR flow curves (i.e. 10–15 Pa). The up and the down curves were measured without any intermediate step. For both ramps the measuring time was 200 s. The oscillatory measurements were performed primarily based on CS results, after that, the measurements were completed by varying stress and frequency. The Creep-Recovery analyses were conducted by using plate-plate rotor at different stress values maintaining for 60 s and then removed after the same time (60 s). Temperature was maintained constant at  $25\text{ }^{\circ}\text{C}$  during the experiments. Rheological parameters were analyzed by Haake software RheoWin 3.61.0004.

Small ceramic discs with 1.5 cm in diameter were obtained by slip casting suspensions prepared at different conditions on plaster of Paris moulds.<sup>7</sup> The green densities of the disc-shaped specimens was determined by mercury immersion technique (Poresizer 9320, Micromeritics, USA) after drying at room conditions for 48 h. Shaped discs were sinterized at  $1600\text{ }^{\circ}\text{C}$  for 1 h in a vertical furnace (LindbergBlue, USA). The densities values were determined by using the Archimedes' principle. All densities values were reported as percentage of theoretical density ( $T_d$ ) of alumina ( $3.99\text{ g cm}^{-3}$ ).

### 3. Results and discussion

Fig. 1 shows the SEM micrograph of the  $\alpha\text{-Al}_2\text{O}_3$  powders. Lamellar particles it can be observed with some variation of particle size ( $0.25\text{--}3.5\text{ }\mu\text{m}$ ). Morphology and the particle size are important because directly influence the rheological behavior<sup>4</sup> of the high solid concentrated suspensions.

The alumina Zeta potential curve is showed in Fig. 2. The literature reports the isoelectric point occurs around pH 9.0,<sup>4</sup> and the stability values ( $>20\text{ mV}$ ) are observed at pH below 7.5 and above 11.5. In concentrate suspensions, the citric acid amount (0.2 wt.%), added as dispersant,<sup>5</sup> promotes a  $\sim\text{pH } 5$ , and according to the results presented in Fig. 3, it is showed Zeta potential value sufficient to obtain stable suspensions.

The effect of dispersants with a low molecular weight, such as citric acid, is based mainly on the charging of the surface of powders particles, thereby increasing the repulsive double-layer forces. The steric hindrance caused by the adsorption of these small molecules is negligible.<sup>5</sup> Thus, the small size of

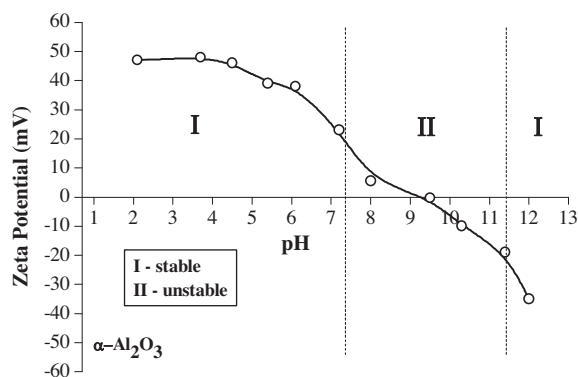


Fig. 3.  $\alpha\text{-Al}_2\text{O}_3$  zeta potential curve.

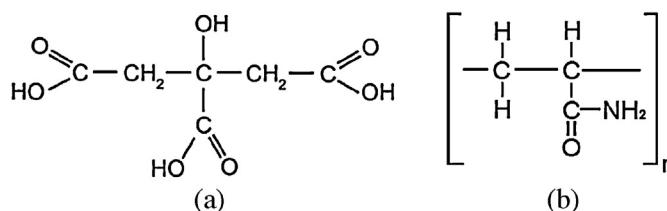


Fig. 4. Citric acid (a) and polyacrylic acid ammonium salt (b) molecules.

citric acid molecule, allows a better insight about interparticle forces, compared to ammonium salt of a polyacrylic acid ( $\text{NH}_4\text{-PAA}$ ), a polymeric dispersant (polyelectrolyte) commonly used in ceramic processing (Fig. 4). Polymers can induce interparticle repulsion and colloidal stability when they are grafted or adsorbed onto the particles. The  $\text{NH}_4\text{-PAA}$  molecule has an average molecular weight of 2400 Da, i.e. molecules length enough to promote viscoelastic responses at interparticle forces level when the solids content in suspension are high. The dispersant amount required to produce stable suspensions, are 0.2 wt.% for citric acid and 0.8 wt.% for  $\text{NH}_4\text{-PAA}$ ,<sup>8,9</sup> both related to the dry solids. It is possible to achieve stability with citric acid by using 25 wt.% of needed  $\text{NH}_4\text{-PAA}$  amount, hence, the molecule interference expected, in interparticle forces responses, are also lower with citric acid.

The alumina suspensions flow curves, with different solid contents, are shown in Fig. 5. It can be observed as expected an increase in flow resistance and a change of behavior, from shear-thinning to shear-thickening (dilatancy), due to solids loading increment.

The transition shear-thinning to shear-thickening, with solid content increase, are displaced to lower shear rates (Fig. 6), starting at shear rate of  $50\text{ s}^{-1}$  in suspensions with 43 vol.%. This change is similar to that observed for kaolin concentrate suspensions.<sup>10</sup> The increasing of viscosity observed in kaolin suspensions from  $400\text{ s}^{-1}$ , is attributed “house of cards” structure formed by the difference of the electrostatic charge between the edges and faces of kaolin particles, which have platelet shape. In the alumina suspensions this behavior is attributed to lamellar morphology of the alumina particles, observed in Fig. 1, likewise the particle size ( $0.67\text{ }\mu\text{m}$ ),<sup>4</sup> associated with high solids concentration.<sup>11</sup>

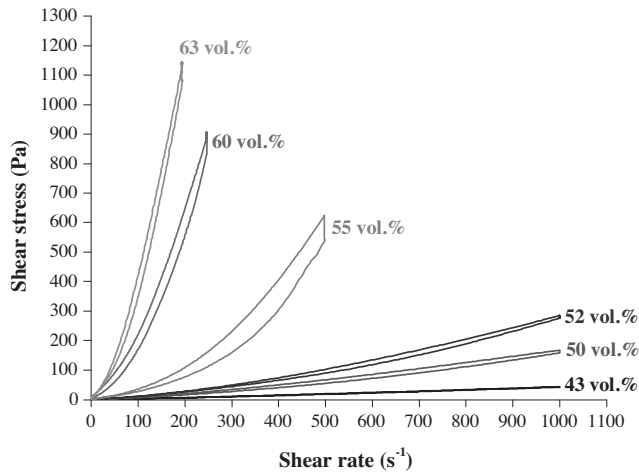


Fig. 5. Flow curves for suspensions with different solids loading, obtained in CR mode.

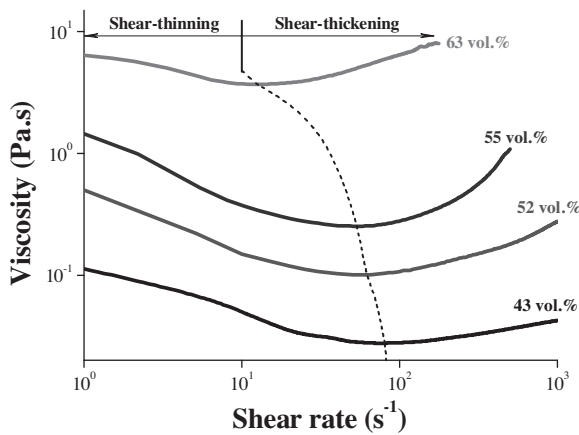


Fig. 6. Viscosity curves versus shear rate highlighting the transition shear thinning to shear thickening, for alumina suspensions with different solids loading.

Analyzing the rheological behavior by CS mode for all studied suspensions, it was possible to measure the yield stress showing as deformation versus stress curves, both in log scale.<sup>4</sup> The yield stress observed at Fig. 7 occurs only for 60 and

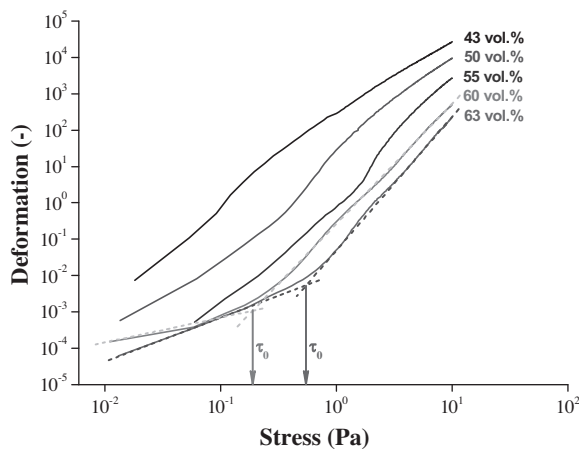


Fig. 7. Deformation versus stress curves for alumina suspensions with different solids loading, attained by CS mode.

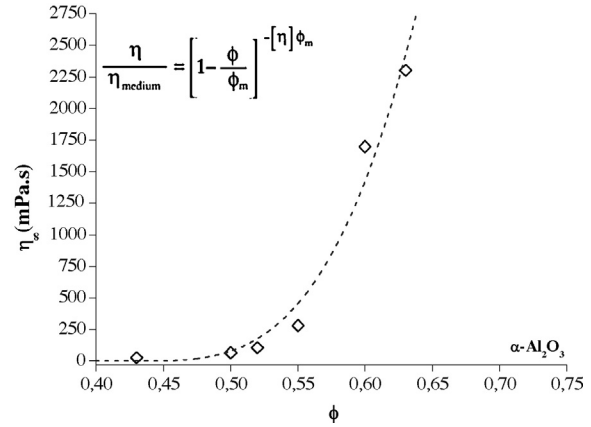


Fig. 8. Variation of viscosity of alumina suspensions with volume fraction of solids.

63 vol.% solid content suspensions. These means that below this stress values, suspensions cannot flow, similar behavior can be observed in Bingham fluids.<sup>3,4,11,12</sup> This behavior indicates that interparticle forces can be active, because of the small distance between ceramics particles. Above these values the suspensions flow. For these measurements be reproducible, they must be executed in same conditions. Yield stress values measured were 0.2 and 0.5 Pa, respectively.

In this study, the Cross model was used because of it can properly predict the general form of flow curves by introducing values of the limit viscosity extrapolated to zero shear rate ( $\eta_0$ ) and infinite shear rate ( $\eta_\infty$ ) providing important and accurate information on the behavior conditions of high and very low shear rates, near the resting conditions.<sup>4</sup>

Fig. 8 shows the variation of relative viscosity as a function of the volume fraction of solids ( $\eta_\infty - \phi$  curves) of the milled suspensions, calculated in the high shear rate region by fitting the experimental  $\eta_\infty$  data (symbols) to the Krieger-Dougherty model (line),<sup>13</sup> where  $\phi_{\max}$  values up to 0.65 were found, quite close to maximum solids loading used in this work.

Rheological analyses for all studied suspensions are presented in Table 1. All parameters have been increased with solid content, as expected. Negative values of thixotropy, determined by rheometer software, are due to shear-thickening behavior from the shear rate of  $80.3 \text{ s}^{-1}$ . Although it not observed large areas in flow curves between the up and down curves, the difference is due to the fact of the rheometer software considers the full extent of measurement. The values of dynamic viscosity at  $10 \text{ s}^{-1}$  have been considered since this is the value generally achieved by casting in plaster Paris moulds (slip casting). Concentrate suspensions showed viscosities values in terms of  $2000 \text{ mPa.s}$  at  $10 \text{ s}^{-1}$ , in other words, sufficiently fluids for slip casting shaping.<sup>14,15</sup> Thus, as can be observed, the suspensions with 60 and 63 vol.% were not been suitable to be shaped by this technique. The yield stress, as early mentioned, only appear in the two last studied conditions. These results are the bases beginning to start a viscoelastic behavior study. The other rheological parameters determined are coherent with the solid contents.

Table 1  
Alumina suspensions rheological properties.

Solid content (vol.%)	Cross model parameters		Thixotropy (Pa s <sup>-1</sup> )	Viscosity at 10 s <sup>-1</sup> (mPa s)	Yield stress (log–log curves – Pa)	Shear-thinning to shear-thickening transition (s <sup>-1</sup> )
	Viscosity at 0 s <sup>-1</sup> (mPa s)	Limite viscosity (mPa s)				
43	54.8	26.3	–889.5	48.5	–	80.3
50	17,010.0	65.7	–8761.0	103.4	–	70.2
52	28,550.0	106.5	–8742.0	150.1	–	60.3
55	49,570.0	280.6	–20,460.0	383.9	–	55.4
60	4841.0	1698.0	–5420.0	2183.0	0.2	32.7
63	12,080.0	3375.0	–77,590.0	3730.0	0.5	12.6

### 3.1. Viscoelastic analyses

Based on yield stress values observed in Fig. 6, the viscoelastic parameters could be determined. Only for 60 and 63 vol.% solids produced suspensions, the viscoelastic parameters were measured. Determination of the linear viscoelastic region was the first step. In this region involves both viscous and elastic properties. However, under a applied stress, the response of the material has been kept constant even though linear region/range. To obtain this behavior range, the oscillatory analyzes are ought to be adequate. These measurements were performed keeping constant the frequency, and the applied stress varied. As the ceramic materials do not show plastic behaviors, except clays, high frequencies do not lead a suitable control, changes can occur very quickly, and all of these factors prevent the accuracy analysis of the involved phenomena. In the other hand, low frequencies take too long time for results to be acquired. Thus, 0.5 Hz was used in this study and the obtained results has been very satisfactory. These analyses are presented in Figs. 9 and 10.

Increasing solids content, the interparticle average gap remarkably decreases, limiting the Brownian movement and promoting attractive interactions by London-van der Waals forces. This implies an increased tendency to develop a structure of particles in the suspension, which results in greater elasticity.<sup>4</sup>

In Fig. 9, it is observed the 63 vol.% alumina suspension has a tendency to linearity below 0.6 Pa. The determination of

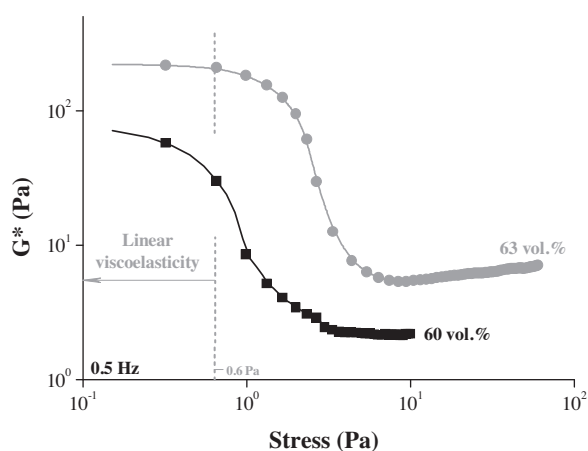


Fig. 9. Oscillatory measurements varying applied stress at 0.5 Hz constant frequency.

these parameters is not trivial, since their behavior is completely unlike polymeric materials or suspensions with polymeric additives (binders, plasticizers, etc.), it not has long chain organic in its composition. The complex modulus ( $G^*$ ) are composed by two components: solid-like component at no particular frequency is characterized by the storage modulus,  $G'$ , and the liquid-like response is described by the complementary loss modulus,  $G''$ . Normally, in polymeric materials or suspensions, the stress values achieved are higher than these observed. However, these promote valuable subsidies to suitable comprehension of ceramic suspensions interparticle interaction. For 60 vol.% alumina suspensions, the linear viscoelastic point could not be determined. Likely, the interparticle forces are not sufficient intense and thus, the linear viscoelastic behavior not occurs.

Results achieved from results shown in Fig 9, the components solid-like and liquid-like,  $G'$  and  $G''$  moduli are respectively presented in Fig. 10. Both are at high solid content suspensions conditions, but the storage modulus ( $G'$ ) only occurs, for ceramic suspensions, when the interparticle distances are very close. From this figure (Fig. 10) it can be observed a behavior changing, for 60 vol.% alumina suspensions, at 0.9 Pa and, for 63 vol.%, at 2.5 Pa. The components intersection point is denominated crossover. Below 0.9 Pa, the alumina suspension with 60 vol.% solids content show an storage modulus domains, after this point the loss modulus (viscous liquid) overlap the elastic component and above 2.5 Pa, the solid-like component

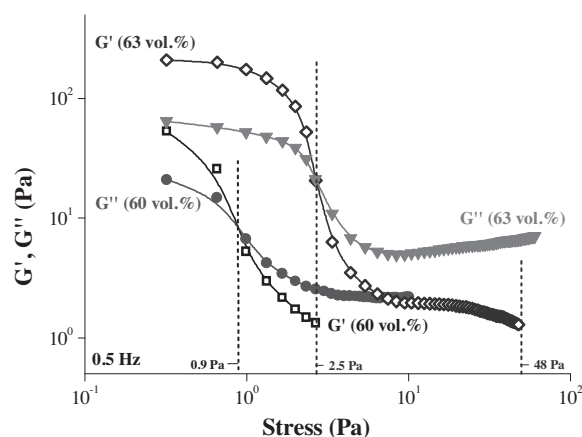


Fig. 10.  $G'$  and  $G''$  versus applied stress curves at 0.5 Hz constant frequency.

Table 2  
Crossover data for high solid content alumina suspensions.

	60 vol.%	63 vol.%
$G' = G''$ (Pa)	11.7	22.5
$\sigma$ (Pa)	0.9	2.5
$\gamma$ (-)	0.087	0.087

thoroughly disappears. The same analyses for 63 vol.% alumina suspensions show a viscoelastic behavior up to 48 Pa. The storage component predominance occurs up to 2.5 Pa, after this, the loss modulus overlaps the solid-like condition and flow behavior dominates the rheological response. These above information are important for plastic shaping as injection, pressing and extrusion because, at low stress conditions, a part of applied deformation can be recovered. The recovery behavior analyses are presented forward, with creep-recovery curves resulted from both 60 and 63 vol.% solid content suspensions. The crossover data for both analyzed suspensions are presented in Table 2.

Fig. 11 shows the oscillatory analyses performed at linear viscoelastic range for 63 vol.% alumina suspensions. As predicted, the viscoelasticity was increased with frequency rise. The extrapolated measured data can be distributed into six excerpts, except for section IV, the others divisions has been similar those found in the literature.<sup>3</sup> The explanation of these sections is presented below.

- (I) The viscous region, where  $G''$  predominates and viscous (flow) behavior prevails. All materials have this region, even solids, because they creep at long times.
- (II) The transition-to-flow region is so called because, when viewed from higher frequencies (where elastic behavior dominates and  $G' > G''$ ), the loss modulus  $G''$ , describing viscous or flow behavior becomes significant. The point where the two moduli crossover is noted as relaxation time ( $\tau_r$ ), given by the inverse of the crossover frequency ( $\tau_r = 2\pi/\omega$ ). Hence, for 63 vol.% alumina suspension, the relaxation time is 22.4 s.

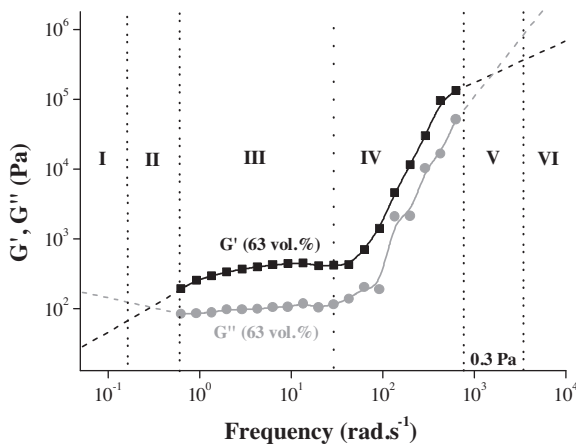


Fig. 11.  $G'$  and  $G''$  versus frequency curves attained at linear viscoelastic range for 63 vol.% alumina suspension.

- (III) The plateau (or rubbery) region is that elastic behavior dominates. The value of  $G''$  is always lower than that of  $G'$ . Plateau modulus ( $G_p$ ) can often be identified in the region where the modulus  $G'$  is almost constant. In this region the material exhibits constant behavior, i.e. the response of the material has been regardless of stress time applied.  $G_p$  modulus found 430 Pa.
- (IV) The increase both moduli with frequency in this specific region occurs due to the “house of cards” structure formed by the difference between the electrostatic charge edges and faces of alumina particles which have platelet shape. The same behavior is observed in Fig. 6.
- (V) The higher transition crossover region has been observed. The value of  $G''$  again rises due to high-frequency relaxation and dissipation mechanisms, at this time faster than  $G'$ . Once more at  $G' = G''$ , a crossover frequency can be defined, and another characteristic time can be obtained. The second crossover happens at  $1550 \text{ rad s}^{-1}$ .
- (VI) This region is denoted as glassy region, in which  $G''$  again predominates and continues to rise faster than  $G'$  and viscous (flow) behavior prevails. From this point, the solid-like component tends to disappear.

Oscillatory measurements, when inflicted cross the linear viscoelastic region, show also liquid-like and solid-like components. However, their analyses are different those observed in Fig. 11. When the applied load are under crossover, as observed in Fig. 10, the elastic component prevail at low frequencies, up to the elastic component stops to exist by increasing the frequency without crossing the elastic and viscous components. For strains over the crossover (Fig. 10), at low frequencies, the viscous component is predominant, but increasing the frequencies, as early mentioned, the elastic component disappears. For higher loads the frequencies in which the solid-like disappears it has been reduced. The conjunction of low frequency and low stress are preponderant to achieve viscoelastic properties in high solid content ceramic suspension. This behavior can be observed in Fig. 12(a) and (b), for 60 and 63 vol.% alumina suspensions, respectively.

Based on viscoelastic results, illustrated in Fig. 10, the recovery response was attained by creep-recovery analysis for 60 and 63 vol.% alumina suspensions. The Fig. 13 shows in detail the creep response for 63 vol.% suspension at 0.3 Pa and its parameters. It can be observed three distinct regions; the first is attributed to immediate elastic response, the second section has both elastic and viscous components and the third region have only a viscous response. The three regions observed correspond to Burger viscoelastic model (Fig. 14), a combination from two simple mechanical models, Kelvin-Voigt and Maxwell,<sup>3</sup> and therefore the analysis could properly be performed. All analyses realized on viscoelastic region showed some recovery. For high solid concentration suspensions the ratio of recovery strain over applied strain is a function only of the applied strain, not of the time, and thus, the time to attain the results can be shorter than polymer materials.<sup>16</sup> The creep-recovery parameters presented in Fig. 13 are: elastic deformation ( $\gamma_e$ ), recovery deformation ( $\gamma_r$ ) and shear rate ( $\dot{\gamma}$ ). The Burger equation parameters shown in

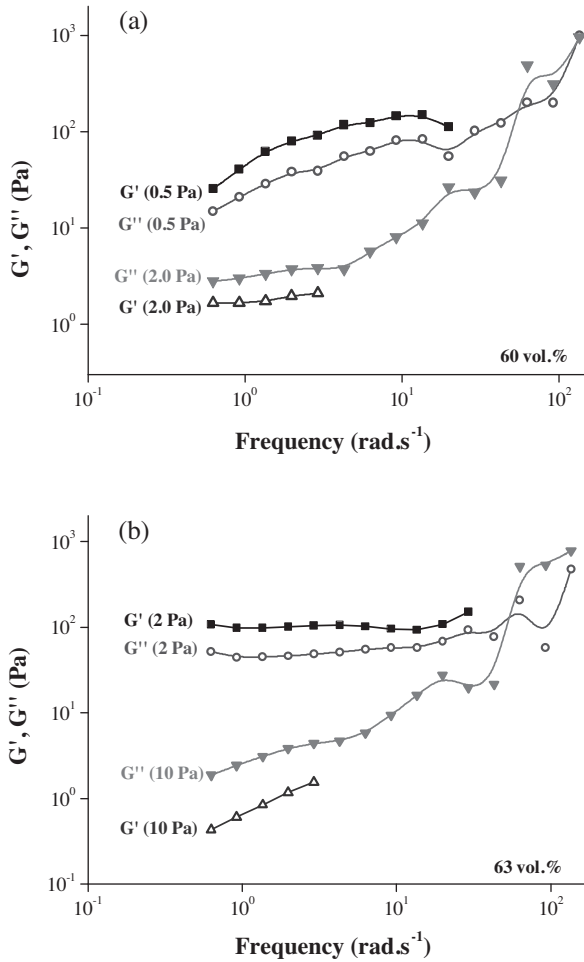


Fig. 12.  $G'$  and  $G''$  versus frequency curves attained at viscoelastic range for 60 vol.% (a) and 63 vol.% (b) alumina suspension.

Fig. 14 are: elastic modulus ( $G$ ), viscosity ( $\eta$ ), deformation ( $\gamma$ ), stress ( $\sigma$ ) and retardation time ( $\lambda$ ).

In Fig. 15(a and b) the creep-recovery curves from 60 vol.% suspension up to different stress values have been shown. Deformations are increased with increment applied strain, as expected.

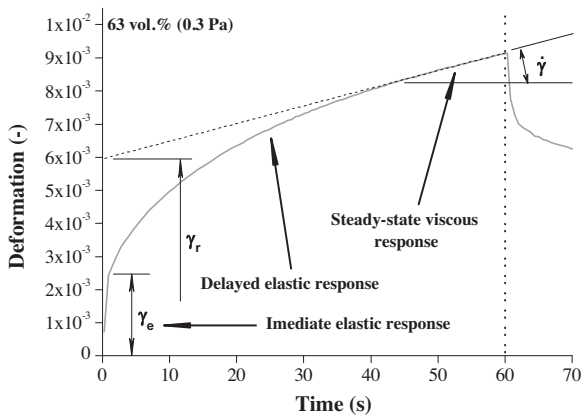
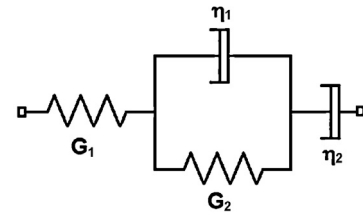


Fig. 13. Creep-recovery curve detailing Burger model for 63 vol.% alumina suspension at 0.3 Pa strain.



$$\frac{\gamma(t)}{\sigma} = \frac{1}{G_1} + \frac{1}{G_2} (1 - e^{-t/\lambda}) + \frac{t}{\eta_1}$$

Fig. 14. Mechanical Burger model and equation.

When applied stress achieves the elastic limit, as observed in Fig. 10, the recovery became negligible (Fig. 15b).

Fig. 16 presents creep-recovery curves for suspensions with 60 and 63 vol.% solids content. It can be observed that the same applied strain, the suspension less concentrated indicates lower resistance deformation and increasing stress and this behavior is more pronounced.

The complete creep-recovery analyses, by using Burger model, for both 60 and 63 vol.% alumina suspensions, at several stress applied, has showed in Table 3. It can be noted that at the

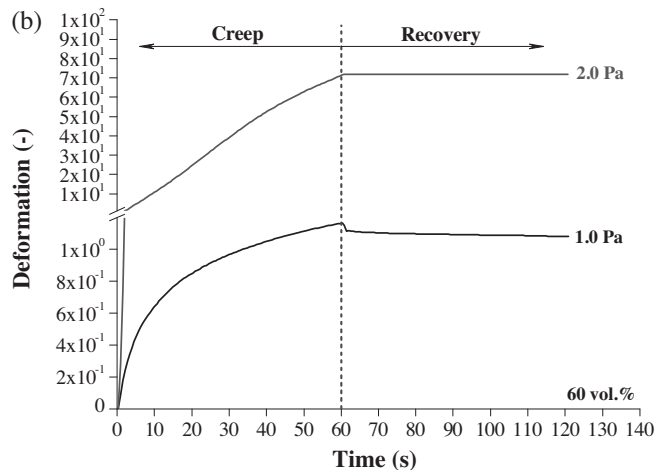
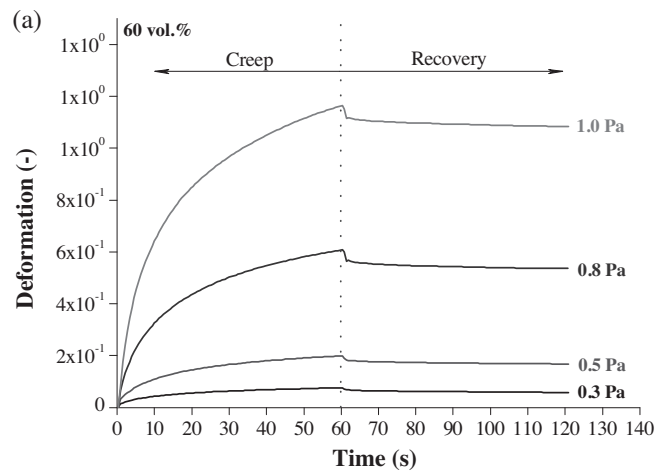


Fig. 15. Creep-recovery curves for 60 vol.% alumina suspensions.

Table 3  
Creep-recovery analyses for 60 and 63 vol.% alumina suspensions solid content, at several applied stress.

	0.3 Pa	0.5 Pa	0.8 Pa	1.0 Pa	2.0 Pa	3.0 Pa
<b>60 vol.%</b>						
$\eta_0$ (Pa.s) <sup>a</sup>	1080.0	617.0	324.1	217.7	2.444	1.140
$\dot{\gamma}$ (1/s)	0.0003	0.0008	0.0025	0.0046	0.8185	2.631
$\gamma_{e0}$ (–) <sup>a</sup>	0.0578	0.1508	0.4596	0.8896	22.360	–
$\gamma_r$ (–)	0.0175	0.0313	0.0719	0.0824	0.1198	–
Recovery (%)	23.20	15.71	11.84	7.08	0.17	–
$\lambda_0$ (s) <sup>a</sup>	195.7	186.1	186.2	193.7	27.3	–
$G_0$ (Pa) <sup>a</sup>	5.52	3.32	1.74	1.12	0.09	–
<b>63 vol.%</b>						
$\eta_0$ (Pa.s)	6573.0	5759.0	5772.0	4972.0	1969.0	673.8
$\dot{\gamma}$ (1/s)	0.0004	0.0001	0.0001	0.0002	0.0010	0.0045
$\gamma_{e0}$ (–)	0.0063	0.0080	0.0239	0.0341	0.2584	0.2420
$\gamma$ (–)	0.0037	0.0036	0.0098	0.0127	0.0362	0.0643
Recovery (%)	40.77	31.48	30.36	27.55	11.34	6.474
$\lambda_0$ (s)	128.3	145.0	172.4	169.4	254.5	163.1
$G_0$ (Pa)	51.22	39.72	33.47	29.36	7.74	4.13

<sup>a</sup>  $\eta_0$  index means  $t = 0$ .

same strain values, suspension with more solid content shows higher recovery values and as the load applied is increased, the suspensions recovery is reduced. Over elastic limit, no more recovery can be found. The recovery values must be considered in plastic shaping processes at low stresses therefore they can influence the final dimensions of the products. In general, all determined parameters are proportional at each studied condition.

These results discussed are derived from interparticle interactions, the higher solids content the particles are closer, more intense are the attraction and repulsion (London-van der Waals) forces active and therefore more responses are pronounced. However, because there are not polymeric chains in these studied suspensions, all viscoelastic responses are located in low stress and strain.

The relative densities of all green pieces shaped presented values of  $\sim 70 T_d\%$ . Independent of the fraction of solids it was possible to obtain similar products. The difference in solids content directly influences the speed of shaping and drying processes, then, is always seeking a middle ground, forming a quick

Table 4  
Relative green and sintered at 1600 °C/1 h densities.

Solid content (vol.%)	Solid content (wt.%)	Green density ( $T_d\%$ )	Sintered density ( $T_d\%$ )
43	75	70.0 ± 0.6	98.9 ± 0.1
50	80	70.1 ± 4.2	99.0 ± 0.1
52	81	70.4 ± 0.7	99.2 ± 0.2
55	83	70.4 ± 1.8	98.8 ± 0.2
60	85	70.4 ± 3.8	98.7 ± 0.2
63	87	69.8 ± 2.5	98.6 ± 0.3

but sufficient to allow an adequate dimensional control of the product.

Density values after sintering (1600 °C/1 h) were high as expected, because of the good green densities values early achieved. The products are suitable, dense and homogeneous. All densities values are presented in Table 4.

#### 4. Conclusions

The alumina suspensions with high solid loading, exhibit a transition from shear-thinning to shear-thickener flow attributed to the lamellar morphology of the  $\alpha$ -Al<sub>2</sub>O<sub>3</sub> particles and also the particle size (0.67  $\mu$ m). Up to 60 vol.% solid content, the alumina suspensions presents viscoelastic behavior that could be determined from oscillatory and creep recovery methods. Higher content of solids promote more intense responses, attributed to interparticle forces, but only in small efforts and deformations.

#### Acknowledgements

The authors are gratefully acknowledged to FAPESP (2009/54851-6), MCT/FINEP/CNPq (142855/2005-7) and CAPES (4710-06-1) for financial and scholarship support. The authors also thank to DSc. Chieko Yamagata and MSc. Mavaiel Jose da Silva, for their collaboration.

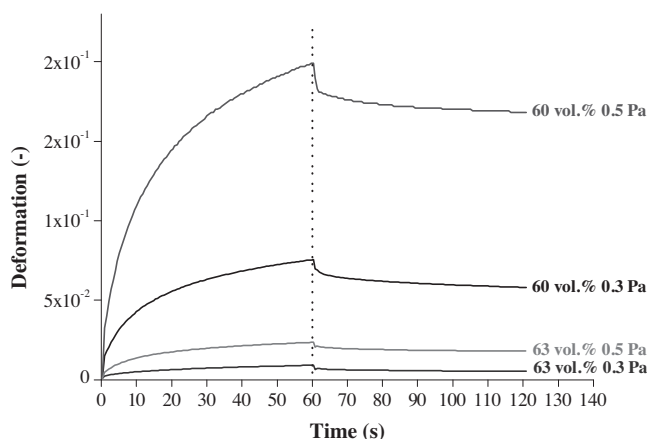


Fig. 16. Creep-recovery curves for both 60 and 63 vol.% solid content suspensions.



## References

1. Ribeiro MJ, Ferreira JM, Labrincha JA. Plastic behaviour of different ceramic pastes processed by extrusion. *Ceram Int* 2005;**31**: 515–9.
2. Barnes HA, Hutton JF, Walters K. *An introduction to rheology*. 1st ed. Oxford: Elsevier Science; 1989.
3. Barnes HA. *A Handbook of elementary rheology*. Aberystwyth: University of Wales – Institute of Non-Newtonian Fluid Mechanics; 2000.
4. Moreno R. *Reología de suspensiones cerámicas*. Madrid: Consejo Superior de Investigaciones Científicas; 2005.
5. Hidber PC, Graule TJ, Gauckler LJ. Citric acid – a dispersant for aqueous alumina suspensions. *J Am Ceram Soc* 1996;**79**:1857–67.
6. Setz LFG, Koshimizu L, Mello-Castanho SRH, Morelli MR. Rheological analysis of ceramics suspensions with high solids loading. *Mater Sci Forum* 2012;**727–728**:646–51.
7. Carvajal A, Moreno R. Estudio de algunas propiedades de los moldes de escayola para el colaje de materiales no arcillosos. *Bol Soc Esp Ceram V* 1988;**27**:11–5.
8. Gutiérrez CA, Moreno R. Preventing ageing on Al<sub>2</sub>O<sub>3</sub> casting slips dispersed with polyelectrolytes. *J Mater Sci* 2000;**35**:5867–72.
9. Sánchez-Herencia AJ, Hernández N, Moreno R. Rheological behavior and slip casting of Al<sub>2</sub>O<sub>3</sub>–Ni aqueous suspensions. *J Am Ceram Soc* 2006;**89**:1890–6.
10. Ferrari B, Moreno R, Lange YFF. Colloidal behavior of a dehydrated kaolin. *Bol Soc Esp Ceram V* 2000;**39**:229–35.
11. Dinger D. *Rheology for ceramists*. 1st ed. Dennis R. Dinger; 2003.
12. Tadros TF. *Rheology of dispersions: principles and applications*. 1st ed. Weinheim: Wiley-VCH; 2010.
13. Setz LFG, Santacruz I, Colomer MT, Mello-Castanho SRH, Moreno R. Tape casting of strontium and cobalt doped lanthanum chromite suspensions. *J Eur Ceram Soc* 2010;**30**:2897–903.
14. Reed JS. *Principles of ceramics processing*. 2nd ed. New York: Wiley-Interscience; 1995.
15. Richerson DW. *Modern ceramic engineering: properties, processing, and use in design*. 2nd ed. New York: Marcel Dekker; 1992.
16. Mewis J, Wagner NJ. *Colloidal suspension rheology*. 1st ed. New York: Cambridge University Press; 2012.